Supporting Information

Water-Soluble Nonconjugated Polymer Nanoparticles with Strong Fluorescence Emission for Selective and Sensitive Detection of Nitro-Explosive Picric Acid in Aqueous Medium

Shi Gang Liu [†], Dan Luo [†], Na Li [†], Wei Zhang [‡], Jing Lei Lei [§], Nian Bing Li [†]*, and Hong Qun Luo [†]*

[†] Key Laboratory of Eco-environments in Three Gorges Reservoir Region (Ministry of Education), School of Chemistry and Chemical Engineering, Southwest University, Chongqing 400715, P.R. China

[‡] Chongqing Institute of Green and Intelligent Technology, Chinese Academy of Sciences, Chongqing 400714, P.R. China

[§] School of Chemistry and Chemical Engineering, Chongqing University, Chongqing 400044, P.R. China

*Corresponding authors: Fax: (+86)23-6825-3237; Tel: (+86)23-6825-3237

E-mail addresses: linb@swu.edu.cn, luohq@swu.edu.cn

Contents

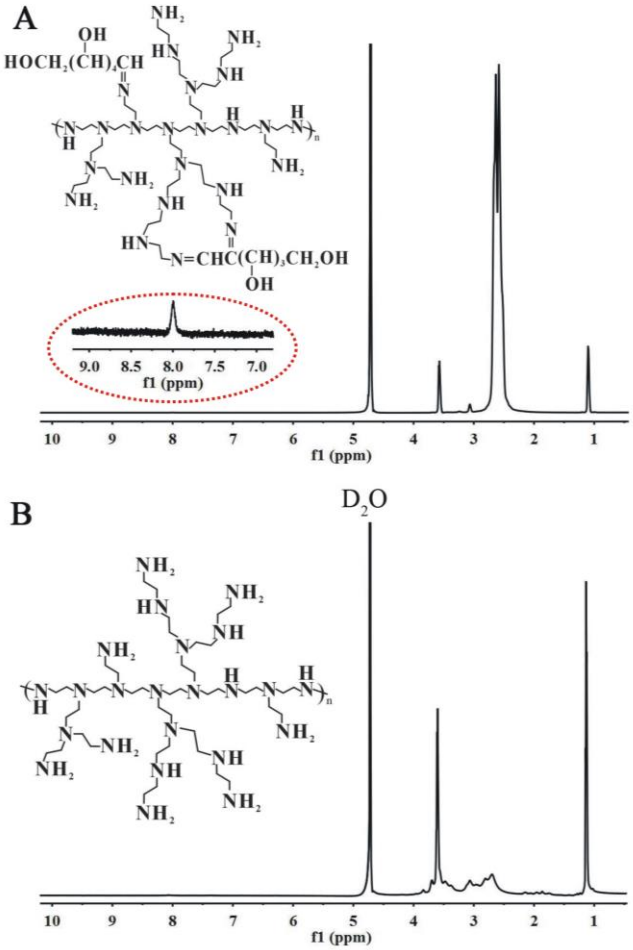

Figure S1. ^{1}H NMR spectra of PEI-G PNPs (A) and PEI (B) (D_2O, 600 MHz). Inset of A is a partial expansion of ^{1}H NMR spectrum of PEI-G PNPs.

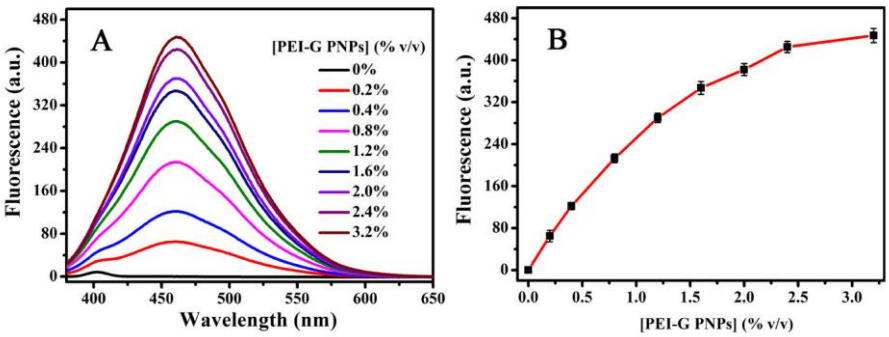

Figure S2. Concentration-dependent fluorescence of PEI-G PNPs. Excitation: 345 nm.

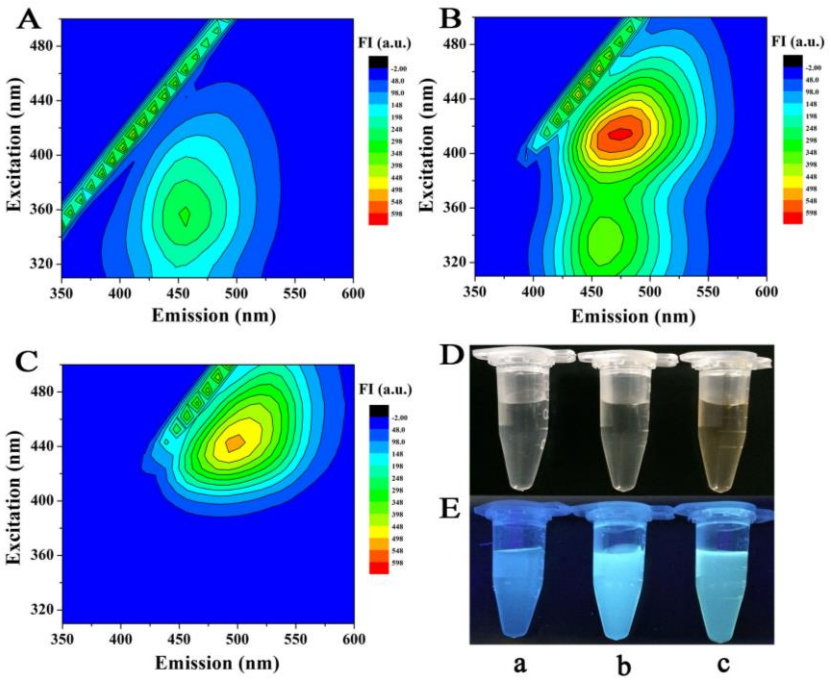

Figure S3. 3D fluorescence spectra of PEI-G PNPs with the concentrations (v/v) of 2% (A), 5% (B), and 10% (C), respectively; and photographs of PEI-G PNPs with the concentrations (v/v) of 2% (a), 5% (b), 10% (c) under visible light (D) and UV light of 365 nm (E), respectively.

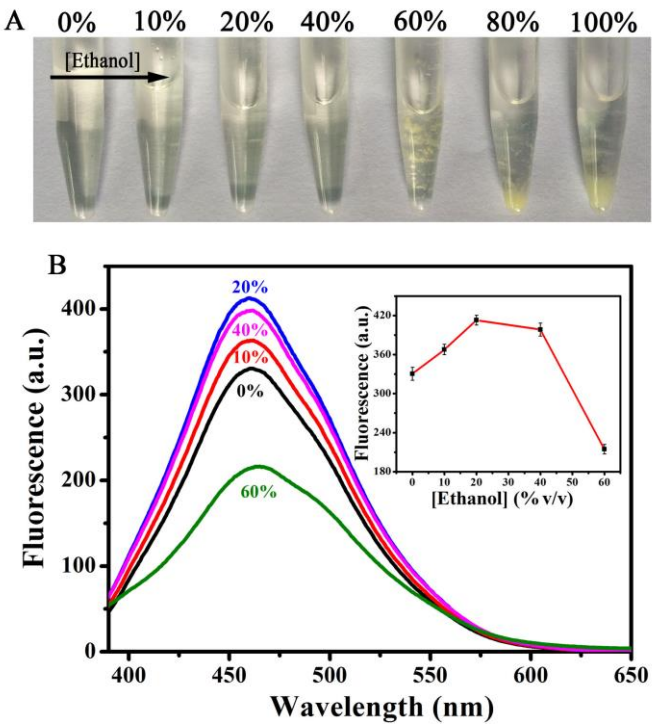

Figure S4. Photographs (A) and fluorescence spectra (B) of PEI-G PNPs (2% v/v) dispersed in an aqueous alcoholic solution with various ethanol contents.

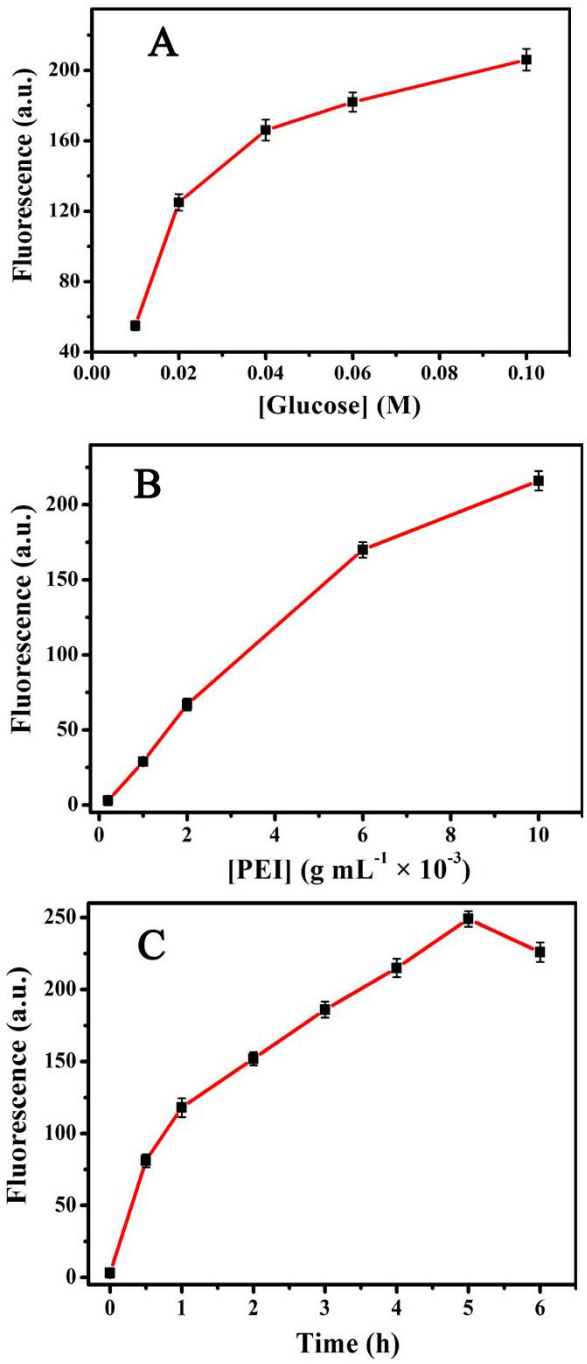

Figure S5. Effects of preparation conditions including the concentration of D-glucose (A), the concentration of PEI (B), and reaction time (C) on the fluorescence intensity of PEI-G PNPs (1% v/v). Conditions: (A) PEI (0.01 g mL^{-1}), 80 °C, 4 h; (B) D-glucose (0.1 M), 80 °C, 4 h; (C) D-glucose (0.1 M), PEI (0.01 g mL^{-1}), 80 °C.

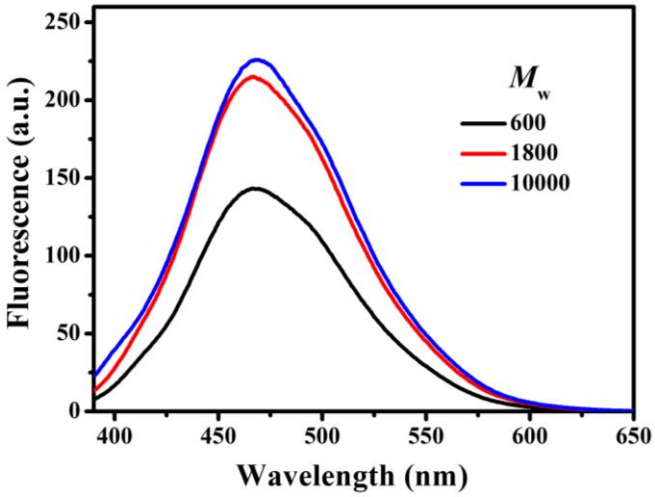

Figure S6. Fluorescence emission spectra of PEI-G PNPs (1% v/v) prepared by using same concentration of PEI with different molecular weights (M_w) with an excitation of 345 nm.

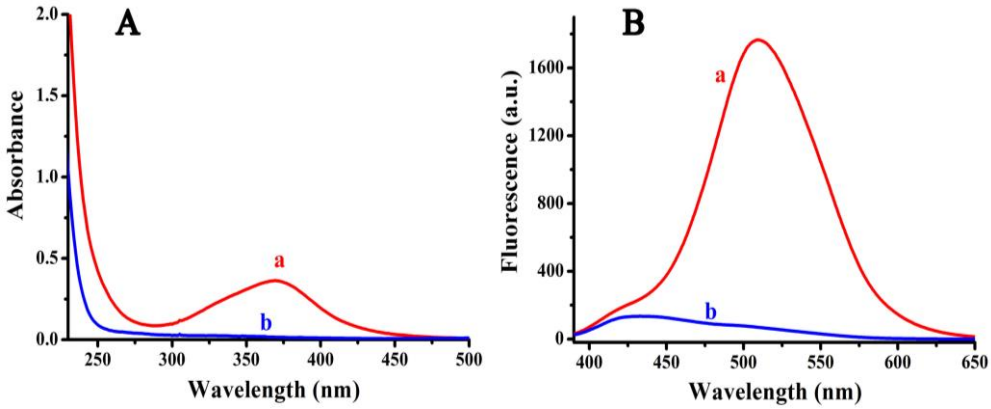

Figure S7. (A) UV-vis absorption spectra of PEI-formaldehyde polymer particles before (a) and after (b) reduced by $NaBH_4$. (B) Fluorescence emission spectra of PEI-formaldehyde polymer particles before (a) and after (b) reduced by $NaBH_4$.

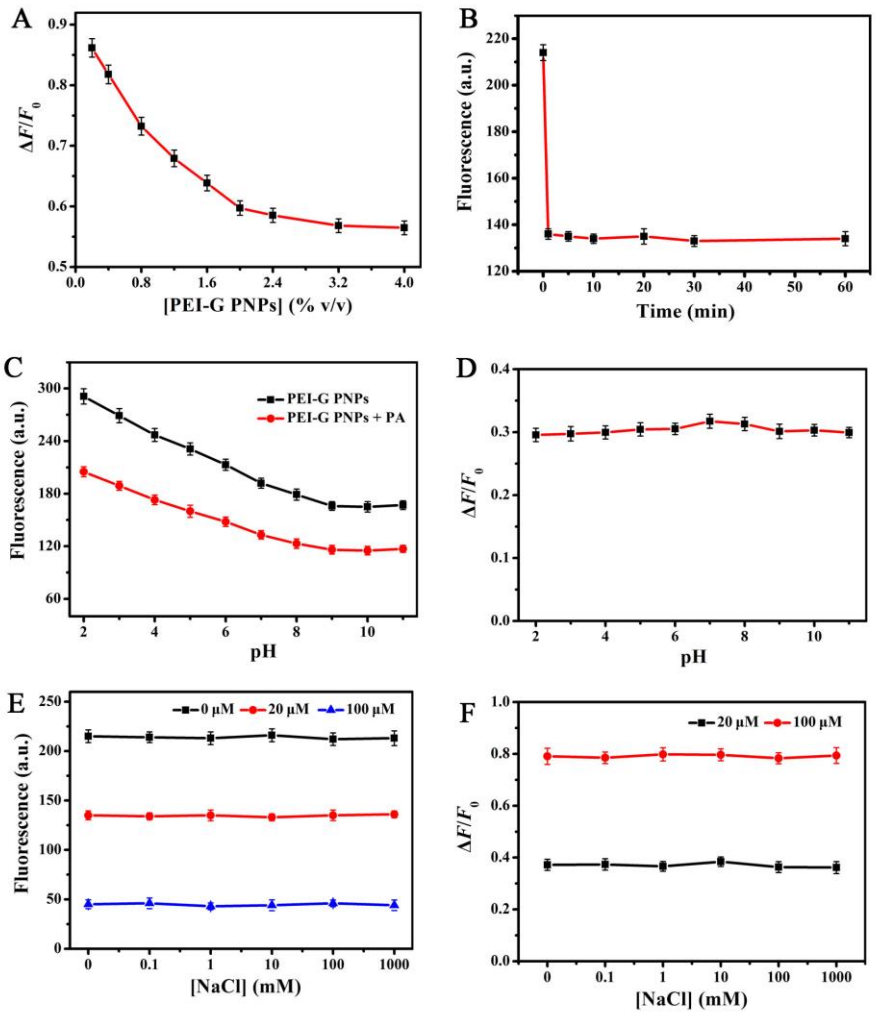

Figure S8. Optimization of sensing conditions. (A) Fluorescence-quenched efficiency of PA (60 μM) to different probe concentrations. (B) Fluorescence response to time upon addition of PA (20 μM). (C) Fluorescence intensities of PEI-G PNPs in the absence and presence of PA (20 μM) under different pH, respectively. (D) Fluorescence-quenched efficiency of PA (20 μM) at different pH (BR buffers). (E) Fluorescence intensities in the absence and presence of PA (20 and 100 μM) at different concentrations of NaCl. (F) Fluorescence-quenched efficiencies of PA (20 and 100 μM) at different concentrations of NaCl.

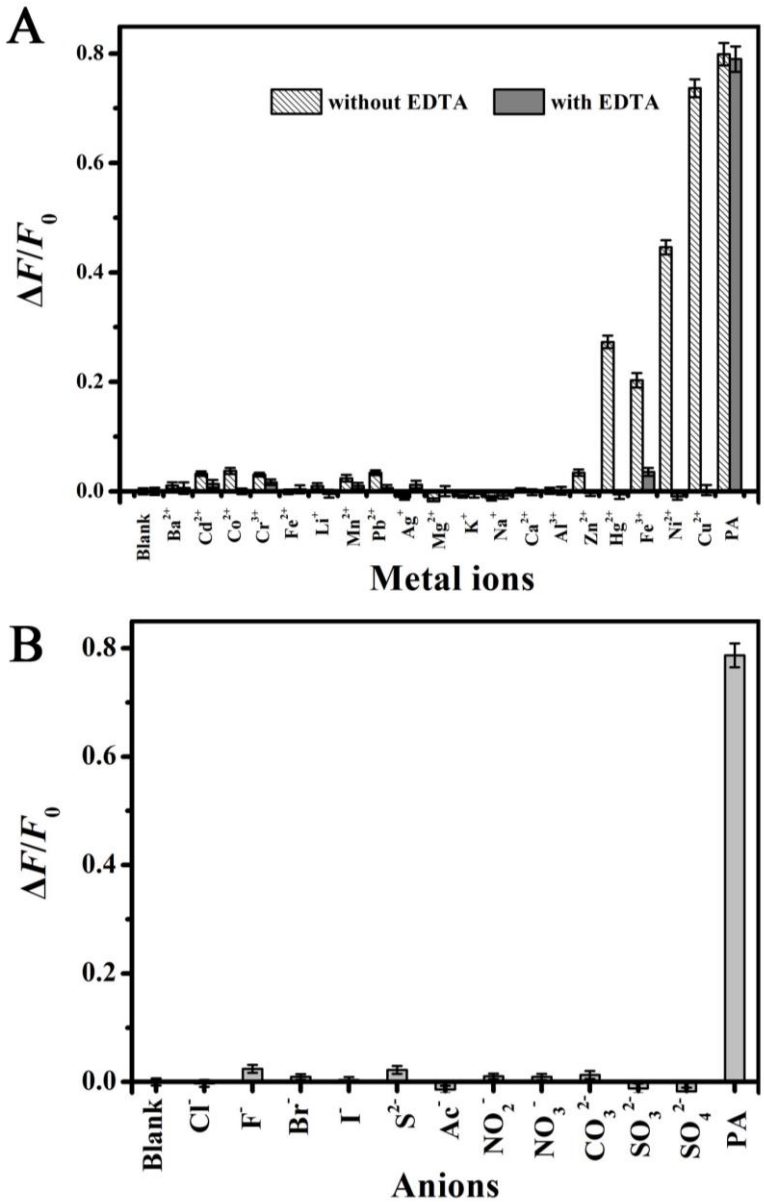

Figure S9. Fluorescence responses of PEG-G PNPs to metal ions in the absence and presence of EDTA (A) and anions (B), respectively. $\Delta F = F_0 - F$, where F_0 and F denote the fluorescence intensity of PEI-G PNPs before and after the addition of ions, respectively. The concentration of all the ions is 50 μM, and the concentration of PA is 100 μM. Conditions: the PEG-G PNPs, 1% (v/v); pH 7.0 (BR buffer).

Table S1. Comparison of fluorescent sensors for PA detection in preparation and analysis.

Material	Preparation	Detection of PA			Ref.
		Linear range (μM)	Detection limit (μM)	Medium used	
MoS_2 quantum dots	200 °C, in water	0.099 – 36.5	0.095	Water	S1
Cu nanoclusters	55 °C, in water	0.8 – 100	0.12	Water	S2
Carbon dots	180 °C, in water	Not given	0.01	Water	S3
Carbon dots	Microwave, in water	Not given	1	Water	S4
Grapheme oxide (GO)	Strong acid	Not given	~ 0.55	Water	S5
MOFs	Multistep, in organic solvents	0 – 50	2.5	DMA	S6
Conjugated polymers	Multistep, in organic solvents	Not given	1	Water/THF (v/v = 9:1)	S7
Covalent-organic polymer	80 °C, in DMF	Not given	~ 4.37	Methanol	S8
Small molecule	Multistep, in organic solvents	0 – 10	0.5	Ethanol	S9
Small molecule	Multistep, in organic solvents	0 – 1	0.28	Water/THF (v/v = 7:3)	S10
Small molecule	110 °C, in toluene	Not given	~ 0.87	Water	S11
Small molecule	Multistep, in organic solvents	0.01 – 0.07	0.0135	Water	S12
Metal complex	Multistep, in organic solvents	Not given	Not given	Water/acetone (v/v = 9:1)	S13
PEG-G PNPs	**80 °C, in water**	**0.05 – 70**	**0.026**	**Water**	**This work**

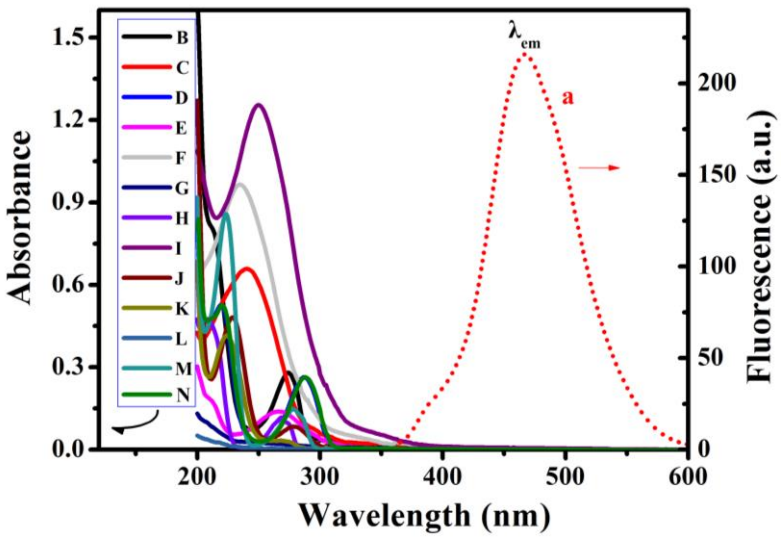

Figure S10. UV-vis absorption spectra of *o*-dihydroxybenzene (B), *m*-dinitrobenzene (C), 4-methylphenol (D), nitrobenzene (E), 2,4-dinitrotoluene (F), *p*-nitrotoluene (G), phenol (H), 2,4,6-trinitrotoluene (I), aniline (J), benzoic acid (K), *o*-nitrophenol (L), *p*-chlorophenol (M), and *p*-dihydroxybenzene (N), and fluorescence emission spectrum of PEI-G PNPs (1% v/v) (a).

Table S2. Detection of PA in environmental water samples using the developed sensor (n = 6).

Sample [a]	Concentration		Recovery (%)	RSD
	Added (μM)	Detected (μM)		(%)
tap water 1	0	ND[b]	/	/
tap water 2	0.5	0.53	106.0	3.37
tap water 3	5	5.18	103.6	2.16
tap water 4	20	20.08	100.4	1.05
Jialing River water 1	0	ND	/	/
Jialing River water 2	0.5	0.56	112.0	4.52
Jialing River water 3	5	5.27	105.4	2.37
Jialing River water 4	20	20.17	100.9	1.13

[a] The tap water was collected from our lab.

[b] ND, not detected.

References

(S1) Wang, Y.; Ni, Y. Molybdenum Disulfide Quantum Dots as a Photoluminescence Sensing Platform for 2,4,6-Trinitrophenol Detection. *Anal. Chem.* **2014**, *86*, 7463-7470.

(S2) Deng, X.; Huang, X.; Wu, D. Förster Resonance-Energy-Transfer Detection of 2,4,6-Trinitrophenol Using Copper Nanoclusters. *Anal. Bioanal. Chem.* **2015**, *407*, 4607-4613.

(S3) Sadhanala, H. K.; Nanda, K. K. Boron and Nitrogen Co-doped Carbon Nanoparticles as Photoluminescent Probes for Selective and Sensitive Detection of Picric Acid. *J. Phys. Chem. C* **2015**, *119*, 13138-13143.

(S4) Niu, Q.; Gao, K.; Lin, Z.; Wu, W. Amine-Capped Carbon Dots as a Nanosensor for Sensitive and Selective Detection of Picric Acid in Aqueous Solution via Electrostatic Interaction. *Anal. Methods* **2013**, *5*, 6228.

(S5) Dinda, D.; Gupta, A.; Shaw, B. K.; Sadhu, S.; Saha, S. K. Highly Selective Detection of Trinitrophenol by Luminescent Functionalized Reduced Graphene Oxide through FRET Mechanism. *ACS Appl. Mater. Interfaces* **2014**, *6*, 10722-10728.

(S6) Shi, Z. Q.; Guo, Z. J.; Zheng, H. G. Two Luminescent Zn(II) Metal-Organic Frameworks for Exceptionally Selective Detection of Picric Acid Explosives. *Chem. Commun*. **2015**, *51*, 8300-8303.

(S7) Liu, Y.; Gao, M.; Lam, J. W. Y.; Hu, R.; Tang, B. Z. Copper-Catalyzed Polycoupling of Diynes, Primary Amines, and Aldehydes: A New One-Pot Multicomponent Polymerization Tool to Functional Polymers. *Macromolecules* **2014**, *47*, 4908-4919.

(S8) Sang, N.; Zhan, C.; Cao, D. Highly Sensitive and Selective Detection of 2,4,6-Trinitrophenol Using Covalent-Organic Polymer Luminescent Probes. *J. Mater. Chem. A*

2015, *3*, 92-96.

(S9) Venkatramaiah, N.; Kumar, S.; Patil, S. Fluoranthene Based Fluorescent Chemosensors for Detection of Explosive Nitroaromatics. *Chem. Commun*. **2012**, *48*, 5007-5009.

(S10) Ding, A.; Yang, L.; Zhang, Y.; Zhang, G.; Kong, L.; Zhang, X.; Tian, Y.; Tao, X.; Yang, J. Complex-Formation-Enhanced Fluorescence Quenching Effect for Efficient Detection of Picric Acid. *Chem. Eur. J.* **2014**, *20*, 12215-12222.

(S11) Yadav, A.; Boomishankar, R. Concentration Dependent Ratiometric Turn-On Selective Fluorescence Detection of Picric Acid in Aqueous and Non-Aqueous Media. *RSC Adv.* **2015**, *5*, 3903-3907.

(S12) Gogoi, B.; Sen Sarma, N. Curcumin–Cysteine and Curcumin–Tryptophan Conjugate as Fluorescence Turn On Sensors for Picric Acid in Aqueous Media. *ACS Appl. Mater. Interfaces* **2015**, *7*, 11195-11202.

(S13) Hou, X. G.; Wu, Y.; Cao, H. T.; Sun, H. Z.; Li, H. B.; Shan, G. G.; Su, Z. M. A Cationic Iridium(III) Complex with Aggregation-Induced Emission (AIE) Properties for Highly Selective Detection of Explosives. *Chem. Commun*. **2014**, *50*, 6031-6034.